Journal of Energy Storage 21 (2019) 202–215

Contents lists available at ScienceDirect

Journal of Energy Storage

journal homepage: www.elsevier.com/locate/est

The experimental evaluation of lithium ion batteries after flash cryogenic freezing

Thomas R.B. Grandjean*, Jakobus Groenewald, James Marco

Energy and Electrical Systems, WMG, University of Warwick, Coventry, CV4 7AL, UK

ARTICLE INFO

Keywords:
Lithium ion battery
Waste battery transportation
Circular economy
Reverse logistics
Remanufacturing

ABSTRACT

The reverse logistic challenge of transporting waste automotive lithium ion battery (LIB) packs is an escalating concern as the world-wide sale of electric vehicles (EVs) continues to rise. Under the European Union (EU) Battery Directive, EV manufacturers are classified as battery producers and are responsible for the collection, treatment and recycling of waste or damaged vehicle batteries. The European agreement concerning the International Carriage of Dangerous Goods by Road (ADR) stipulates that damaged or defective LIB packs must be transported in approved explosion proof steel containers. This necessitates costly testing in order to meet ADR requirements. Furthermore, the extra size and weight of this packaging adds further prohibitive expense to the transportation of damaged or defective LIB. In this study, cryogenically frozen cells are shown to be unable to release any energy even in extreme abuse conditions. This is demonstrated on two different cell chemistries and form factors. Experiments have shown that the possibility of thermal runaway is completely removed and therefore it is argued that LIBs may be transported safely whilst cryogenically frozen. Moreover, flash freezing is shown to have little effect on the electrical performance (energy capacity and impedance) even after five repetitive cryogenic cycles. Thus, facilitating the potential reuse and remanufacture of individual LIB cells from a complete damaged pack, prolonging the useful life, reducing the consumption of raw materials, and improving environmental sustainability of EV introduction.

1. Introduction

The automotive industry's pursuit to actively reduce its impact on the environment by shifting its dependence from the internal combustion engine (ICE) vehicle to alternative sustainable technologies continues to gain momentum. This shift is occurring amidst an ever increasing framework of legislation to reduce carbon emissions, such as the EU 2020 targets [1] and growing concerns over local air pollution [2–4]. Fuel combustion arising from transport (including international aviation) has increased significantly since 1990 to comprise 23% of all greenhouse gas emissions across the EU in 2015 [5]. The adoption of hybrid electric vehicles (HEVs), plug-in hybrid electric vehicles (PHEV) and battery electric vehicles (BEVs) have the potential to yield considerable greenhouse gas emission reductions [6]. These electric vehicles (EVs) typically contain lithium-ion batteries (LIBs) as the dominant technology due to their relatively high energy density, long life cycles, lack of memory effect, and slower self-discharge rates [7]. Market adoption of LIBs continues to grow; for example the Boston Consulting Group predicts 26% of new cars sold in 2020 will have electric or hybrid power trains and in total 11 million of these vehicles will be equipped with LIBs [8]. Furthermore, Bloomberg New Energy Finance annual long-term forecast estimates that 54% of new cars sold in 2040 will be EVs, underpinned by impending reductions in LIB prices [9].

As discussed in a number of publications [10–12], eventually the LIB inside an EV will no longer be suitable for its original automotive application and will need replacing. The performance of LIBs is known to diminish during usage; important characteristics, e.g. energy capacity and impedance that directly correlate to vehicle range and acceleration attributes, deteriorate due to ageing mechanisms such as solid

Abbreviations: ADR, European Agreement concerning the International Carriage of Dangerous Goods by Road regulations; ANOVA, Analysis of Variance; BEV, battery electric vehicles; CC, constant current; CID, Current Interrupt Device; CV, constant voltage; DK, Dow Kokam; EOL, end of life; EU, European Union; EV, electric vehicle; FSR, Full Scale Range; HEV, hybrid electric vehicles; HPPC, Hybrid Pulse Power Characterisation; HVM, High Value Manufacturing; LIB, lithium ion battery; LN_2, liquid nitrogen; NCA, nickel cobalt aluminium oxide; NMC, nickel manganese cobalt oxide; PTC, Positive Temperature Coefficient; SE, standard error; SOC, State of Charge

* Corresponding author.
E-mail address: T.Grandjean@warwick.ac.uk (T.R.B. Grandjean).

https://doi.org/10.1016/j.est.2018.11.027
Received 11 October 2018; Received in revised form 27 November 2018; Accepted 27 November 2018

electrolyte interphase layer growth [13–15]. End of life (EOL) for automotive applications is generally defined when the battery has suffered 20% capacity fade from new [16] or when the resistance of the cell has increased by a factor of two [17]. EOL may also be reached due to field failures or road traffic accidents which damage the battery pack. EOL protocols such as re-use (see [18] for an example), remanufacturing or recycling are not well established [19,20].

Producing LIBs is known to be highly energy intensive, with production-related emissions estimated in the range of 38–356 kg CO_2-eq/kWh [21]. It is therefore important to extend the useful life of LIB systems as much as possible. However, current legislation such as the European agreement concerning the International Carriage of Dangerous Goods by Road (ADR) [22] and the Battery Directive [23] make it prohibitively expensive to transport damaged and defective batteries which is pre-requisite step before any battery recycling or repurposing may occur. The ADR special provision 376 (SP376) [22] stipulates that "damaged or defective" LIB packs which are hazardous be assigned to transport category 0 and are transported under conditions approved by the competent authority of any ADR Contracting Party. Within this context, hazards include: "liable to rapidly disassemble, dangerously react, produce a flame or dangerous evolution of heat or a dangerous emission of toxic, corrosive or flammable gases or vapours" [22] and therefore must be transported in approved explosion proof steel containers, which are expensive. For example an explosion proof container for a typical Tesla sized pack costs circa €10,000 and the UN accreditation is a further circa €10,000 [24]. The solution proposed here is to freeze LIBs, which would mean the LIB cells are no longer defined as hazardous. The potential arises that if a cryogenically frozen LIB cell can be proven to comply to the requirements of ADR SP376 [22], it would permit safe transport.

The aims of this research are twofold. First, to demonstrate that cryogenically frozen cells cannot release energy or fail catastrophically within the context of subsequent storage or transportation. This would mean that frozen LIBs may not be defined as hazardous and therefore would not need to be transported under damaged LIBs dangerous goods regulations that mandate the use of approved explosion proof containers. The second research aim is to quantify the electrical performance effect of flash freezing Li-ion cells in terms of both their retained energy capacity and internal impedance. Thereby promoting sustainability as undamaged cells and modules within a complete damaged battery pack may be reused or remanufactured. This is timely research as there are considerable articles addressing remanufacturing, repurposing, and recycling of LIB (e.g. [25–29]), however the current reverse logistic of transporting damage and defective batteries has not been considered fully. The "triple win" report by the all-party Parliamentary Sustainable Resource Group and the All-Party Parliamentary Manufacturing Group highlights the social, economic and environmental case for remanufacturing [30]. It asserts that the future of the manufacturing industry is inextricably linked to environmental sustainability, reducing the consumption of raw materials, and exploiting new areas of comparative advantage, and that remanufacturing plays a critical role in this.

This paper is structured as follows: Section 2 provides a detailed analysis of the current legislation relevant to the reserve logistics of waste batteries. Reverse logistic is defined as the process of transporting LIBs from their automotive applications for the purpose of capturing value, or proper disposal. The cell selection and experimental method is described in Section 3. The experimental results are shown in Section 4 and discussed in Section 5, including further work. Finally, the main conclusions from the research are summarised Section 6.

2. Waste battery reverse logistics

2.1. Current legislation and standards

Article 3 (12) of the Battery Directive [23] defines battery producers as any person placing batteries (including those incorporated into EVs) on the market for the first time, i.e. EV manufacturers. The financial responsibility for the reverse logistic of waste automotive traction batteries is placed on battery producers. Furthermore, Article 16 (1) of the Battery Directive [23] imposes the 'principle of producer responsibility', whereby battery producers, or third parties acting on their behalf, must finance any net costs arising from collecting, treating and recycling of all waste *industrial* and automotive waste batteries. The Environment Agency within the United Kingdom (UK), in its guidance on waste batteries [31], classifies LIBs providing the power to drive EVs as industrial batteries. Within this context, automotive batteries are defined as the traditional lead-acid battery type employed for starting, lighting and ignition power requirements in conventional road vehicle engines.

Whilst many cylindrical cell designs contain safety mechanisms, such as Positive Temperature Coefficient (PTC) devices and Current Interrupt Devices (CID), which considerably mitigate risks, thermal runaway remains an important safety concern with the use and transport of LIBs [32–34]. Organic electrolytes, which are based on combinations of linear and cyclic alkyl carbonates, allow the use of lithium as the anodic active component in LIBs [32]. Lithium provides a wide operating voltage (2.5–4.2 V) that gives LIBs their characteristic high power and energy densities. However, the electrically conducting solution has a high flammability and volatility that can pose serious safety issues since it can react with the active electrode materials to release significant heat and gas, such as carbon dioxide, vaporized electrolyte consisting of ethylene and/or propylene, and combustion products of organic solvents [32].

According to the International Energy Agency's Global EV Outlook, the global EV stock surpassed 2 million units in 2016 [35]. As reported within [36], there are considerable challenges to overcome in order to safely implement the reserve logistics of millions of LIBs. Lisbona & Snee [37] assert that the potential severity of incidents during storage, transport and recycling of waste batteries can be significantly higher than that found in end-use applications. Consequently, transporting LIBs by road, rail or sea is subject to dangerous goods legislation [38]. For the purpose of transportation, LIBs are classified by the Environment Agency as Class 9 ("other dangerous goods"). The transport options for EOL LIB under ADR [22] are summarised in the flowchart shown in Fig. 1.

The ADR [22] and the United Nations (UN) Model Regulations on the Transport of Dangerous Goods [39] both stipulate that all LIBs should be tested according to the UN38.3 [40] test methods. LIBs are identified as damaged or defective when they no longer conform to the type tested according to UN38.3 [40]. Fig. 1 shows that, according to ADR [22] if LIBs are not damaged or defective they can be transported under special provision 377 in accordance with packing instruction P909, i.e. packaged in a container conforming to Packing Group II specifications. If the LIBs are damaged or defective (including LIBs that cannot be diagnosed) and deemed safe, they can be transported under special provision 376 in accordance with packing instruction P908 or LP904, i.e. also packaged in a container conforming to Packing Group II specifications. Unsafe LIBs are assigned to transport category 0 and can only be transported in an approved explosion proof container as per ADR SP376 [22]. This necessitates costly testing, as each battery pack needs to be destructively tested inside its proposed container in order to meet ADR requirements, increasing the total packaging cost (e.g. its design, testing and manufacture) to tens of thousands of pounds for many applications. Furthermore, the extra size and weight of the cumbersome packaging adds further expense to the transportation process, which is inherently governed by system weight and volume.

2.2. Supporting LIB recycling and repurposing

The requirement for transporting unsafe LIBs in approved explosion proof containers causes issues for EVs involved in road traffic accidents.

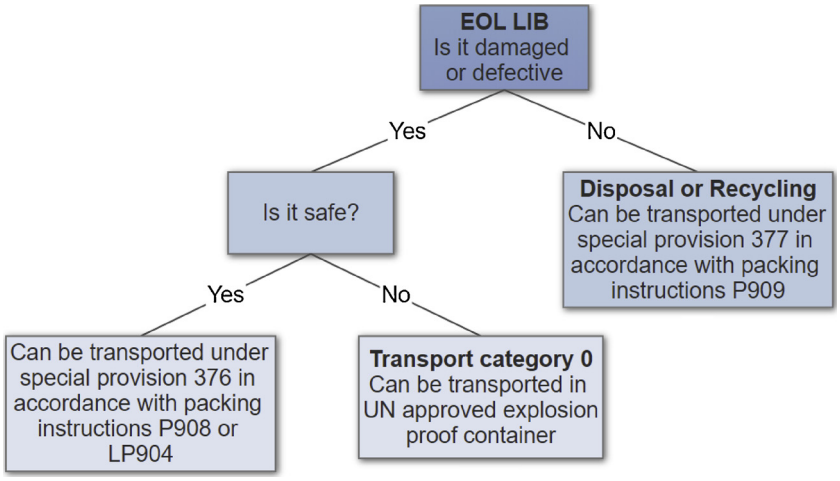

Fig. 1. Flowchart for EOL LIB transport options under ADR [22].

First responder guides [41] recommend removing the 12 V power supply to the LIB pack, which means the battery management system (BMS) is not operational and there is a high probability that the BMS will not be able to establish whether the LIB pack is safe. In line with the requirements of ADR [22], safety in this paper is defined as not being able to explode, vent dangerous gases, catch fire, or go into thermal runaway. In a road traffic accident where the BMS is operational, there is no guarantee that it has not been damaged and is functioning as designed. In reality, it is generally not possible to establish if a damaged or defective LIB is safe since the LIB is not conforming to the type tested according to UN38.3 [40]. It would therefore require additional testing to ensure it is safe, which is not possible to do at a road traffic accident site. It would mean that LIB packs with no or only relatively minor damage might be discarded since it is not economically viable to transport them to a battery re-use or re-manufacturing facility. A large LIB can contain thousands of individual lithium-ion cells and can be rendered damaged or defective by ancillary failures, e.g. a failure of the BMS to report battery status, or a proportion of the cells being damaged or defective. Therefore, in a damaged or defective pack, most of the cells could still be reusable, depending on the failure mode.

Reports of LIBs unexpectedly and spontaneously combusting during storage are not uncommon [42]. Notably, this risk may be minimised by storing LIBs at low temperatures [43]. This approach may also have implications for developing mitigation strategies for accidents during manufacturing and testing. One cell going into thermal runaway can subsequently cause adjacent cells to follow suit. An entire module or pack can be destroyed. This problem and a possible viable solution can potentially have great impact on how the battery waste industry manages risk in the future. Pouring liquid nitrogen on a pack has the potential to halt the cascading effect described [44,45]. Some publications advocate that damaged and leaking LIBs batteries are placed directly into salt water and disposed of as hazardous chemical waste (class 8) [38]. The chloride ions in the salt water form an ionic pathway to slowly discharge the battery and react with Li-ions to form lithium chloride, a stable hydrate salt crystal. However, this method is known to have major disadvantages. Notably, if lithium comes into contact with water, it causes an exothermic reaction which produces hydrogen fluoride, a dangerous colourless gas. Furthermore, the salt water corrodes the cell terminals and it becomes difficult to measure the pack voltage to confirm it is electrically stable and therefore safe. As a result, since the electrolyte is sealed inside individual cells, it is necessary to pierce every single cell to ensure that the battery cannot release any energy, which is normally not possible at pack level. This process is, by definition, destructive and as such, none of the battery components can be reused or remanufactured for possible 2nd-life applications, as discussed within [46]. Finally, the resulting salt-water slurry is highly corrosive and poses an additional environmental disposal challenge.

There a number of different recycling methods that have been proposed to recover lithium from batteries; such as hydrometallurgy [47], hybrid metallurgy [45], and chemical extraction [48]. However, most companies use pyrometallurgy [49]. Despite Sonoc et al. 2015 [44] demonstrating that discharging cells to 0 V in order to open them safely is a more efficient way to recycle, commercial recycling companies such as Retriev technologies Inc. and BDC Inc. use the Toxco process [50]. This involves cryogenically cooling larger waste batteries that might still hold an electrical charge in liquid nitrogen (LN_2) before mechanically hammering and shredding then submerging in water where the lithium ions will react with the water to produce lithium hydroxide and hydrogen gas [44]. Indeed, using cryogenic freezing for safe handling of hazardous materials has been an established process method since the early 90 s [51]. Since recycling processes either involve incineration, smelting or shredding, there are no concerns recycling damaged or defective batteries. The valuable metals, such as cobalt, can still be extracted.

Low ambient temperatures are known to cause significant power losses in LIBs [52] due to reduced electrolyte diffusivity and conductivity [53,54]. As such, researchers have been reformulating electrolyte compositions in attempts to improve the performance of LIBs at low temperatures [55–57]. Despite new mixtures exhibiting a glass transition that takes place at temperatures below − 70 °C, most state-of-the-art electrolytes crystallise at temperatures below − 40 °C [58].

Whilst using LIBs at low temperature is known to cause degradation via ageing mechanisms such as lithium plating of the electrode [59], NMC/graphite lithium-ion pouch cells have been cooled at a constant rate down to − 105 °C [60]. However, it is not clear from the literature, whether flash freezing LIBs to cryogenic temperatures (< − 150 °C) is detrimental since it is has not previously been reported. Flash freezing could cause damage within the cell as materials with different thermal coefficients of expansion; causing internal stresses. Metals (positive electrodes are made of metal oxide) typically exhibit 0.2-0.4% contraction in length when exposed to cryogenic temperatures, whilst organic materials and polymers, such as the separator, will range from 1% to 2.5% contraction [61]. In addition, salt and solvent precipitating at the electrode and density changes from crystallisation of the solvents could cause damage; rapid change around the freezing point is common in organic solvents [62,63]. However, the electrolyte was expected to freeze into a solid solution due to the rapid cooling rate [52].

This work proposes to transport damaged or defective batteries whilst cryogenically frozen, in assessing this alternative approach it is important to consider the implications of the cryogenic system failing during transportation. Since LIB packs have a large thermal mass, it

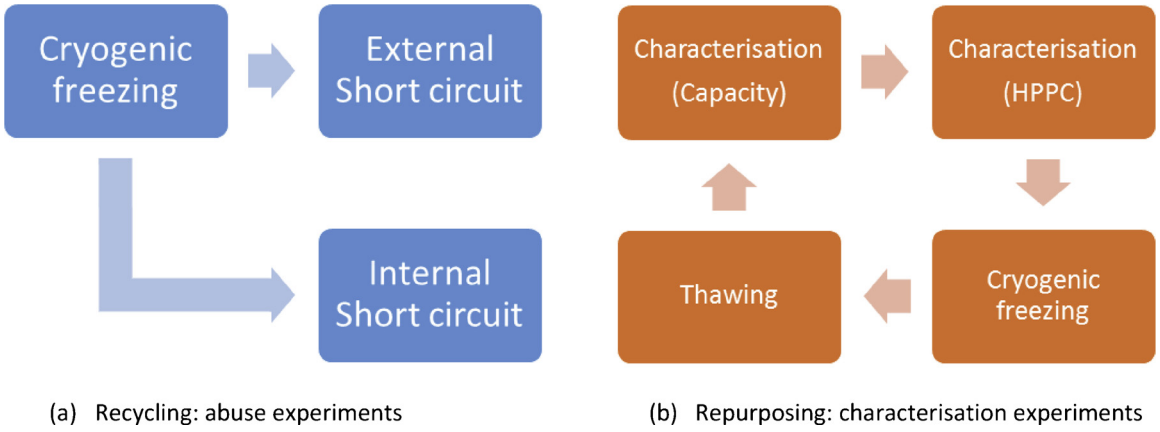

Fig. 2. Process flowchart.

could take days for a cryogenically frozen pack to thaw and become hazardous and thus allow repair of the cryogenic system. Furthermore, insulation can be used to extend the thawing time to ensure the LIB pack will remain unable to go into thermal runaway.

3. Experimental method

As described in Section 2.2, it is desired to insure damaged and defective LIBs are safe using cryogenic freezing in order to facilitate recycling and repurposing because unsafe or unknown LIBs have to be transported in approved explosion proof steel containers. Since a damaged or defective LIB pack may contain a proportion of undamaged cells, it is therefore also desired to demonstrate cryogenic freezing of LIBs is non-destructive, in order to facilitate undamaged cells and modules to be repurposed. The experimental procedures followed in this study have been split into two parts, recycling and repurposing, as shown in Fig. 2.

The first section details the abuse testing performed on the cells to demonstrate safety (defined in Section 2.2) at cryogenic temperature. The second section specifies the characterisation experiments performed to quantify the degradation caused by cryogenic flash freezing. This is done at different states of charge (SOC), as the lithium ions are intercalated in the anode when it is charged and in the cathode when it is discharged. It is assumed therefore that the level of oxidation/reduction of each electrode could affect the results.

3.1. Cell selection

Two different cell formats were selected for evaluation in this study; Dow Kokam (DK) 5 Ah 100 x 106 mm pouch and Panasonic 3 Ah 18,650 cylindrical cells. Table 1 summarises the pertinent electrical performance data for each cell. The pouch cell is manufactured with low internal impedance for power applications such as for use within a HEV, whereas the 18,650 cell is more suitable for energy applications such as BEVs. The internal chemistry of the 18,650 cylindrical cell is comprised of nickel cobalt aluminium oxide (NCA) with a LiC_6 (graphite) anode. Conversely, the pouch power cell is nickel manganese cobalt oxide (NMC). These cells were selected because they cover two chemistries that are currently being commercialised by system integrators and vehicle OEMs. For example, Nissan© have opted for the NMC chemistry within the Leaf whilst Tesla© employs NCA. Similarly, both cell formats are under consideration by a number of automotive OEMs researching the integration of Li-ion battery packs within future HEVs and EVs. The cylindrical 18,650 formats has been used by Tesla© whilst the Nissan Leaf© and BMW i3© employ the pouch option. The use of commercially available chemistries and cell formats in this work ensures the applicability and relevance of the findings with respect to impact on the broader industrial sector.

Table 1
Electrical performance data for both the pouch and 18,650 cell types from manufacturer datasheets.

Parameter	Pouch (Power Cell)	18,650 (Energy Cell)
Nominal energy capacity (Ah)	5	3
Internal impedance (1 kHz AC)	< 5.0mΩ	< 35mΩ
Maximum continuous charge rate	2C	C/3
Maximum continuous discharge rate	4C	3C
Maximum cell voltage (V)	4.2	4.2
Minimum cell voltage (V)	2.7	2.5

3.2. SOC adjustments

SOC adjustments were performed as per the recognised method defined in IEC-62660 [64]. The temperature of an Espec thermal chamber was set to 25 °C and allowed to stabilise for 720 min. The cells were fully charged using a constant current (CC) of C/3 to the upper voltage limit defined by the manufacturer (4.2 V) followed by a constant voltage (CV) phase until the current reduced to 0.1 A. The cells were allowed to rest for 180 min prior to being discharged at 1C to the desired SOC.

3.3. Cryogenic freezing

A subset of both the cylindrical and pouch cells were completely submerged via a hydraulic arm into an all-plastic Dewar flask with 5 L of LN_2 for five minutes. This was to ensure the cells were cryogenically frozen throughout. The experimental apparatus is depicted in Fig. 3.

3.4. Recycling: abuse experiments

The primary purpose of the abuse experiments is to demonstrate that the cells are safe (not being able to explode, vent dangerous gases, catch fire, or go into thermal runaway) when they are cryogenically frozen. It is desired to perform the most aggressive abuse tests on the cells to demonstrate their safety at cryogenic temperature. The eight abuse tests detailed in the UN Model Regulations on the Transport of Dangerous Goods [39] are summarised in Table 2.

Test T.6 and Test T.7 (Table 2) are the most extreme tests, which are expected to result in the destruction of the LIB. The remaining six tests (T.1–5 and T.8) are not designed to induce thermal runway and are therefore not performed within this study. A full description of each cell test strategy is defined in the UN Model Regulations on the Transport of Dangerous Goods [39] and will not be repeated here.

As per Fig. 2, the abuse testing is split into two parts: the first section

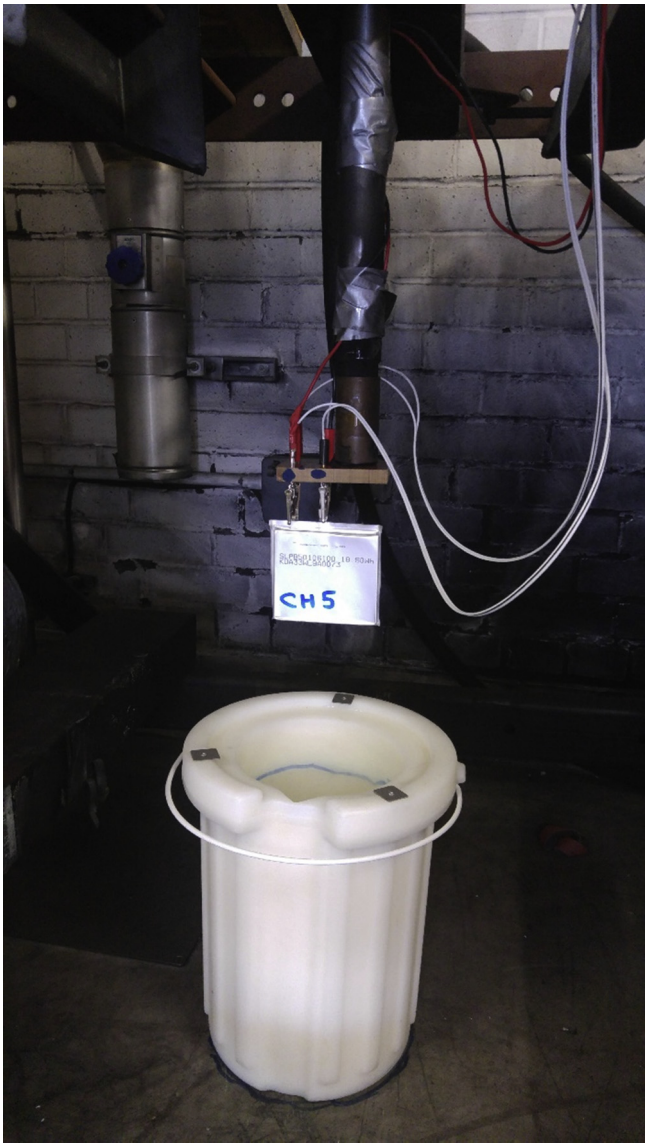

Fig. 3. Photograph of experimental set up with hydraulic arm for submerging Li-ion cells into LN_2.

details the short circuit testing and the second describes the penetration experiments performed. Throughout the experimentation, cell terminal voltage is recorded using a multifunction Maccor 4200 series desktop automated test system, which has a voltage accuracy of ± 2 mV (0.02% FSR – Full Scale Range) and a measurement sampling rate of 10 mS.

3.4.1. Short circuit

In order to ascertain whether the LIBs can release any energy whilst cryogenically frozen, twelve fully charged cells (100% SOC) were subject to an external short circuit. This is achieved by clamping the positive and negative tabs with a 20 mΩ wire at two temperatures: three DK5 Ah were tested immediately after being submerged in liquid nitrogen at −196 °C and another three DK 5 Ah cells were tested at room temperature (15 °C) to provide a benchmark for the typical energy release expected. The experiment was repeated with six Panasonic 18,650 cells. The experiments were performed sequentially in order to mitigate the number of cells that could catastrophically fail simultaneously.

3.4.2. Penetration

One of the most aggressive and destructive tests a cell can endure is where a nail is driven through the cell shorting the electrodes internally [65]. This normally results in an explosive gas release with the potential of fire [66]. A mild steel conductive 20 mm diameter nail, which is electrically insulated from the cell was used. The nail was held perpendicular to the cell with a rate of penetration of 8 cm/sec. The nail was aligned to penetrate directly through the middle of the cell. The nail penetration experiment was performed on six DK 5 Ah cells at two temperatures: three cells were tested immediately after being submerged in liquid nitrogen at −196 °C and the remaining three cells were tested at a room temperature of 15 °C to provide a control sample for the typical energy released.

For the six Panasonic 18,650 cells, during this experiment, the cells were crushed since the cell's metal casing makes it difficult to accurately pierce with a nail. A force was applied to the cell's enclosure until an internal short was achieved.

3.5. Repurposing: characterisation experiments

In order to quantify the degradation caused by cryogenic freezing LIBs, each cell was characterised before and after having been submerged in liquid nitrogen at −196 °C for five minutes and allowed to return to room temperature, circa 15 °C (see Fig. 2). The cells were submerged five times and characterised after 1, 2 and 5 LN_2 submersions in order to determine if the number of submersions affects the results. This experiment was performed with cells at different states of charge (SOC), i.e. 0%, 50%, and 100%, in order to investigate whether this parameter is an important factor. The SOC adjustment procedure is described in 3.2. Sixteen DK 5 Ah cells were used and split into four groups:

1 DK01: cryogenically frozen at 100% SOC (n = 4)
2 DK02: cryogenically frozen at 50% SOC (n = 4)
3 DK03: cryogenically frozen at 0% SOC (n = 4)
4 DK04: control, stored at 20% SOC (n = 4)

A two-factor Analysis of Variance (ANOVA) is performed on all the data in order to establish main effects, i.e. if the SOC and the number of

Table 2
UN Model Regulations on the Transport of Dangerous Goods [39] test manual summary.

Test number	Test name	Purpose
Test T.1	Altitude simulation	This test simulates air transport under low-pressure conditions
Test T.2	Thermal test	This test assesses cell and battery seal integrity and internal electrical connections. The test is conducted using rapid and extreme temperature changes.
Test T.3	Vibration	This test simulates vibration during transport
Test T.4	Shock	This test assesses the robustness of cells and batteries against cumulative shocks.
Test T.5	External short circuit	This test simulates an external short circuit
Test T.6	Impact/Crush	These tests simulate mechanical abuse from an impact or crush that may result in an internal short circuit
Test T.7	Overcharge	This test evaluates the ability of a rechargeable battery or a single cell rechargeable battery to withstand an overcharge condition.
Test T.8	Forced discharge	This test evaluates the ability of a primary or a rechargeable cell to withstand a forced discharge condition.

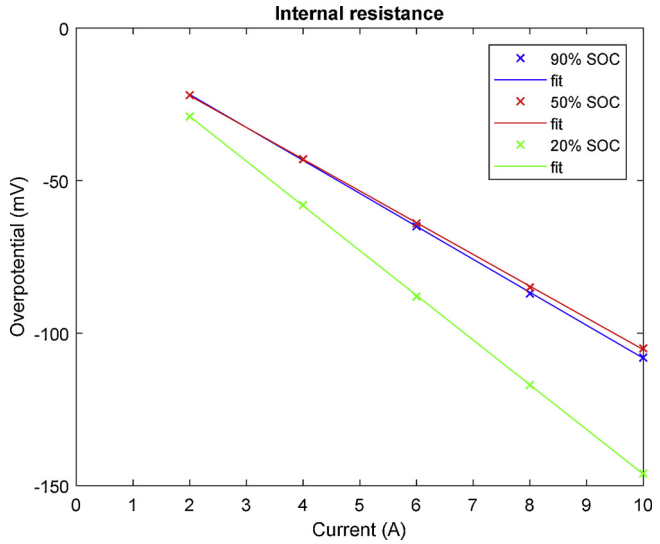

Fig. 4. linear regression of overpotential against current for 5 pulses at 3 SOCs.

LN_2 submersions are statistically significant factors, and the interaction effects between the SOC and the number of LN_2 submersions. Post hoc testing using paired t-tests with Bonferroni correction will be used to analyse statistically significant results.

After all the characterisation experiments on the DK 5 Ah cells had been performed, the experimental method was modified for the Panasonic 18,650 cells. This time 18 cells were used split into four groups:

1 PAN01: cryogenically frozen at 100% SOC (n = 4)
2 PAN02: cryogenically frozen at 50% SOC (n = 4)
3 PAN03: cryogenically frozen at 0% SOC (n = 4)
4 PAN04: control (n = 6): stored at 100% (n = 2), stored at 50% (n = 2), and stored at 0% SOC (n = 2)

Two additional reference cells (PAN04) are used and instead of storing all the control cells at 20% SOC, they are stored at the same SOCs as for the cryogenic freezing (0, 50, and 100% SOC) in order to investigate the interaction between cryogenic freezing and SOC in the reference cells.

Unless otherwise stated, the numerical results presented in Section 4 are a mean-average with error bars representing the standard error (SE) defined as the standard deviation divided by the square root of the sample size.

Cell characterisation, both for the pouch and cylindrical cells, was performed with a multifunction Maccor 4200 series desktop automated test system, which has a current accuracy of ± 7.5 mA (0.05% FSR, a voltage accuracy of ± 2 mV (0.02% FSR), and a sampling rate of 10 mS. An Espec thermal chamber was utilised to control the ambient temperature of the cells at the target temperature of 25 °C to an accuracy of ± 1 °C.

Cell performance was quantified using energy capacity and Hybrid Pulse Power Characterisation (HPPC) measurements, the methodology for which are described in Sections 3.5.1 and 3.5.2 respectively.

3.5.1. Energy capacity

Capacity measurements were performed as per the recognised method defined in IEC-62660 [64]. The temperature of an Espec thermal chamber was set to 25 °C and allowed to stabilise for 720 min. The cells were fully charged using a constant current (CC) of C/3 to the upper voltage defined by the manufacturer (4.2 V) followed by a constant voltage (CV) phase until the current reduced to 0.1 A. The cells were allowed to rest for 180 min prior to being fully discharged at 1C to their respective lower voltage threshold (2.5 V and 2.7 V for Panasonic 3 Ah and DK 5 Ah respectively). The energy extracted from the cells during the discharge was recorded by the Maccor cell cycler as a measure of their 1C capacity. Five "pre-conditioning" capacity measurements are performed sequentially with 3 h rest in prior to cryogenic freezing in order to ensure the cells are functioning as expected. A further three capacity measurements are made after one, two and five LN_2 submersions to investigate the effect of cryogenic freezing on cell capacity.

3.5.2. HPPC

The HPPC results were calculated from 10 pulses (5 charge and 5 discharge) applied at 90%, 50% and 20% SOC at 25 °C after leaving the cells to equilibrate electrochemically and thermally for three hours. This approach is based on the HPPC method defined in IEC-62660 [64].

Since the HPPC is performed at high and low SOC (90 and 20% respectively), it is necessary to modify the pulse amplitudes from IEC-62660 [64] otherwise the cell terminal voltage will exceed the cut-off shown in Table 1. As a result, the maximum discharge pulse at 20% SOC will cause the cell terminal voltage to reach the lower voltage cut-off. Similarly, the maximum charge pulse at 90% SOC will cause the cell terminal voltage to reach the upper voltage cut-off. In both scenarios, the cell cycler automatically reduces the current in order to maintain the cell within the voltage limit. This causes the pulses to be abated, which affects the resulting impedance calculations. This phenomenon is discussed further within [67]. The electrical current values for each of the discharge pulses are 2, 4, 6, 8, and 10 A.

In order to calculate the internal resistance (R_{int}) of the cell, the cell voltage at the end of the 10 s pulse and the corresponding current were recorded for each of the five discharge pulses. The charge pulses are not utilised as typically, LIB internal resistance can be 5–20% higher during charge [68]. The internal resistance R_{int} is estimated using a linear regression of the five pulses, given by

$$R_{int} = \frac{\sum_{i=1}^{n} x_i y_i}{\sum_{i=1}^{n} x_i^2} \quad (1)$$

where x_i is the applied pulse current, y_i is the voltage value after 10 s, n = is the number of pulses, and i is the ith pulse. A graphical representation of Eq. (1) is shown in Fig. 4.

A HPPC characterisation is performed prior to cryogenic freezing as a benchmark. A further three HPPC characterisations are performed after one, two and five LN_2 submersions to investigate the effect of cryogenic freezing on cell impedance.

4. Results

In accordance with the structure of the experimental method defined in Section 3, the experimental results are divided in to two parts: abuse experiments and characterisation experiments to support recycling and repurposing respectively.

4.1. Recycling: abuse experiments

4.1.1. Short circuit

After being submerged in liquid nitrogen at −196 °C, it was observed that the three DK5 Ah cells did not release any energy when a short circuit was applied across the cell terminals, as shown in Fig. 5(a).

The short-circuited DK 5 Ah at room temperature were expected to fail violently (fire and gas release) as the short circuit causes a very rapid discharge. In turn, resulting in a sharp temperature increase that will start to decompose the electrolyte by exothermic reactions causing thermal runaway [69]. However, when the experiment was performed at room temperature (Fig. 5(b)), the three DK5 Ah cells vented gas for a short time period before the heat generated within the cell melted the current collector. Unfortunately, the smoke is not clearly visible in Fig. 5(b).

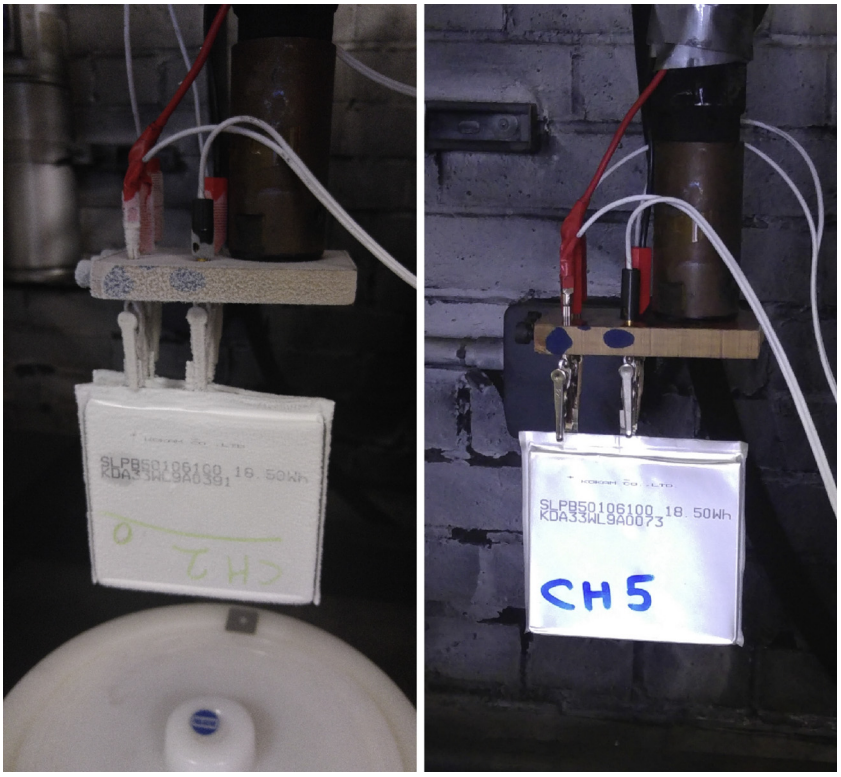

Fig. 5. (a) Cryogenically cooled DK 5 Ah cell perforated with nail compared to (b) same experiment at room temperature.

The cryogenically frozen Panasonic 18650 cells ($n = 3$) did not release any energy when an external short circuit was applied immediately after being submerged in liquid nitrogen at −196 °C. At room temperature, the Panasonic 18650 cells were not expected to fail violently since they are equipped with a Positive Temperature Coefficient (PTC) switch, which prevents high currents inside the cell. A conductive polymer that becomes resistive as it heats up, stops the current flow and protects the cell from external short circuits. When the experiment was performed at room temperature, the Panasonic 18,650 cells heated rapidly until the PTC activated and interrupted the current flow within the cell.

4.1.2. Cell penetration

After being submerged in liquid nitrogen at −196 °C, it was observed that the three DK5 Ah cells did not release any energy when a nail perforated the cells, as shown in Fig. 6(a).

In comparison, when the experiment was performed at room temperature as per Fig. 6(b), all three DK5 Ah cells went into a thermal runaway condition. However, the three Panasonic 18650 cells did not release any energy when they were crushed. Equally, when the experiment was performed at room temperature, the Panasonic cells did not release any energy either. Both of these results are counter intuitive since the safety devices within the cylindrical cells does not protect them against internal short circuits, which cause very high current densities.

4.2. Characterisation experiments

4.2.1. Capacity

The DK 5 Ah and Panasonic 3 Ah capacity average measurements ± SE (as detailed in Section 3.5.1) are presented in Fig. 7. The first five characterisations are prior to cryogenic freezing. The sixth, seventh and eighth characterisations are after one, two and five LN_2 submersions respectivelyHPPC

The DK 5 Ah and Panasonic 3 Ah HPPC average measurements ± SE (as detailed in Section 3.5.2) are presented in Fig. 8. The first characterisation is prior cryogenic freezing. The second, third and fourth characterisations are after one, two and five LN_2 submersions respectively. The characterisations are performed at three different SOCs, 90%, 50%, and 20% shown in Fig. 8(a)–(c) respectively for the DK5 Ah cells. The data are grouped according to the SOC at which the HPPC measurement was performed. For each plot the SOC corresponding to each line is the SOC at which the cells were submerged in LN_2 prior to this test.

5. Discussion

5.1. Recycling: abuse experiments

5.1.1. Short circuit

After being submerged in liquid nitrogen at −196 °C, the three DK5 Ah cells did not release any energy when an external short circuit was applied. The electrolyte was deemed to have frozen and did not permit any ions to mobilise therefore no current could flow within the cell. Conversely, when the experiment was performed at room temperature, it was observed that the three DK5 Ah cells vented gas for a short time period before the heat generated melted the current collector. This effectively acts as an electrical fuse opening a short circuit. Although this prevented the onset of thermal runaway within each cell, this type of failure mode is still deemed to be potentially dangerous since heat and toxic gases are released. The exact composition of the gases released from each cell were not tested but may contain large amounts of toxic hydrogen fluoride and some phosphoryl fluoride, as demonstrated by Larsson et al. [70]. It is noteworthy that if the current collector fails, the cell can no longer be discharged through an electrical connection to the cell tabs and has to be mechanically pierced whilst submerged in a salt bath in order to extract the remaining energy stored to make the cell safe for transportation.

The cryogenically frozen Panasonic 18650 cells ($n = 3$) did not release energy when an external short circuit was applied after being

Fig. 6. (a) Cryogenically cooled DK 5 Ah cell perforated with nail compared to (b) same experiment at room temperature.

submerged in liquid nitrogen at −196 °C. As with the pouch cells, the electrolyte was deemed to have frozen and therefore did not permit ions to mobilise. Conversely, when the experiment was performed at room temperature, it was observed that the Panasonic 18650 cells heated rapidly until the PTC interrupted the current flow. Once the external short circuit was removed and the cell's temperature reduced, the PTC once again allowed cell current to flow. The cell could be discharged using a current 1C, demonstrating the efficacy of the PTC safety device.

In order to simulate thawing after a short circuit occurs during transport, additional experiments were performed where the external short circuit was applied when the cells returned to room temperature after being submerged in liquid nitrogen at −196 °C for five minutes. As the electrolyte began to thaw, the cells were able to conduct a small current. This current flow, in turn, resulted in a small heat build-up to occur. This self-heating accelerated the thawing of the electrolyte and the current flow increased rapidly until the DK5 Ah current collector melted or in the case of the Panasonic 3 Ah the PTC cut off the current. These experiments were repeated with cells at 50% and 20% SOCs, and the results were identical.

5.1.2. Penetration

As for the external short circuit experiment, the electrolyte was deemed to have frozen and did not permit any ions to mobilise therefore no battery current could flow. Interestingly, the cells did not react even after returning to room temperature. The terminal voltage increased to 4.1 V despite the nail still being inside the cell. As the nail was retracted, the DK5 Ah cells caught fire and went into thermal runaway. It is assumed that when the nail penetrated the cryogenically frozen cells it did not cause any internal short circuits as the elastic modulus of the cell materials was greatly increased at cryogenic

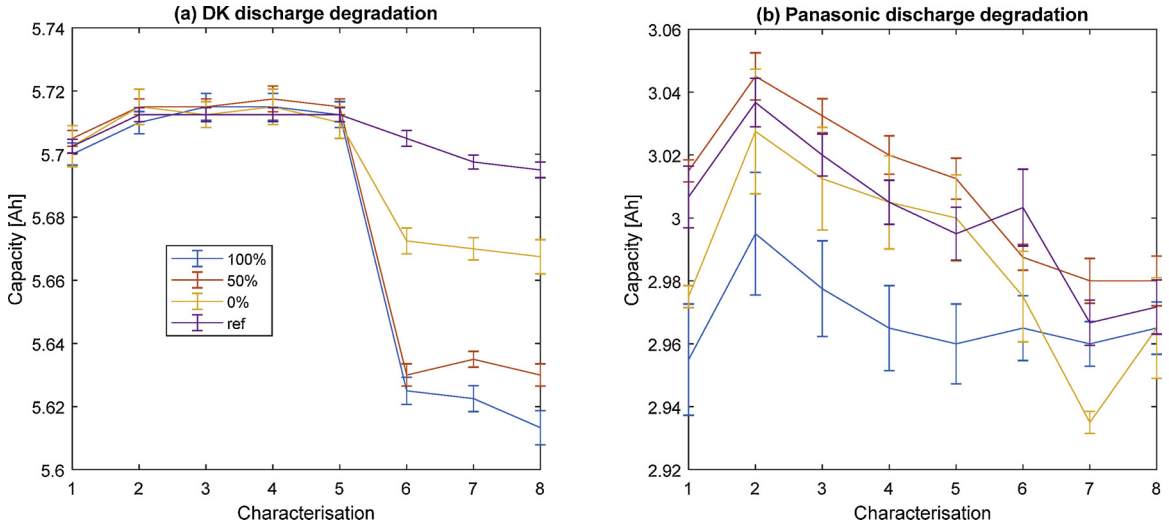

Fig. 7. Capacity measurement of (a) DK 5 Ah cells and (b) Pan 3 Ah at different SOCs (100%, 50%, 0%). Reference cells (purple trace) are not submerged in LN_2 and used to benchmark any degradation due to cryogenic freezing (For interpretation of the references to colour in this figure legend, the reader is referred to the web version of this article).

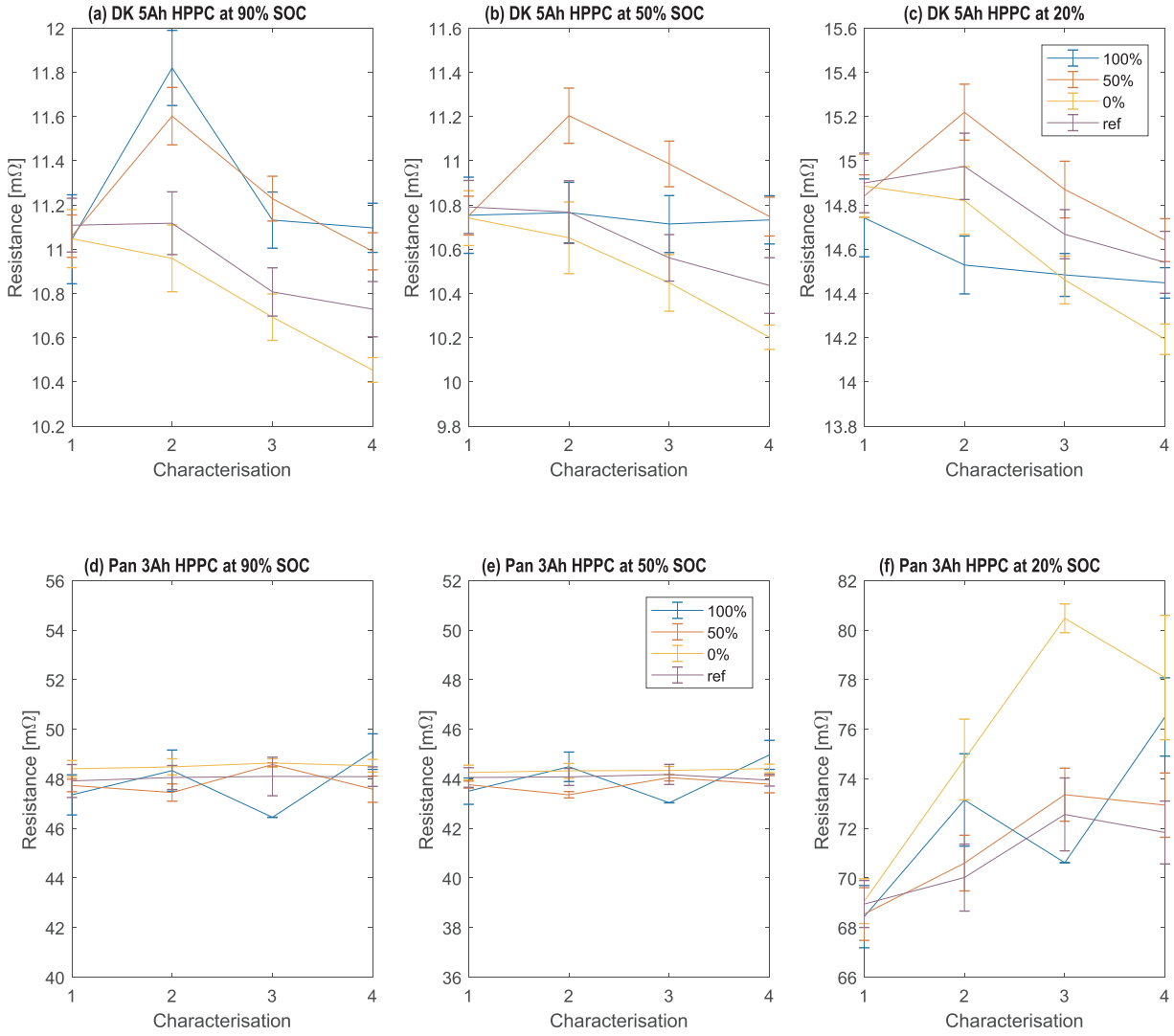

Fig. 8. HPPC measurement of DK 5 Ah cells at (a) 90%, (b) 50%, and (c) 20% SOC, and Pan 3 Ah cells at (d) 90%, (e) 50%, and (d) 20% SOC before and after LN_2 submersions at different SOCs (100%, 50%, 0%). Reference cells are not submerged in LN_2 and used to benchmark any degradation due to cryogenic freezing.

temperature. On the other hand, when it was retracted at room temperature the cell materials had a lower elastic modulus and consequently a short circuit occurred.

Conversely, when the experiment was performed at room temperature, the three DK5 Ah cells caught fire and went into thermal runaway almost immediately after the nail had perforated the cell body. Despite being low energy cells, i.e. 5 Ah capacity, a considerable amount of gases were released as shown in Fig. 6(b), which would be harmful since they are known to contain large amounts of toxic hydrogen fluoride and some phosphoryl fluoride, as demonstrated by Larsson et al. 2017 [70].

Counter intuitively, the three Panasonic 18650 cells did not release any energy when they were mechanically crushed. When the experiment was performed at room temperature (circa 15 °C), the Panasonic cells did not release any energy. It is assumed that the crush damage did not cause penetration of the separator, and therefore an internal short circuit did not occur. A similar result where crush damage is applied perpendicularly to the cell has been reported by Mikolajczak et al. [71].

The abuse experiments demonstrate that both cells types are safe when cryogenically frozen, thereby allowing unknown or unsafe damaged or defective LIBs to be transported in a container conforming to Packing Group II specifications. Since most state-of-the-art electrolytes crystallise at temperatures below − 40 °C, it is suspected that it is not necessary to maintain the packs at cryogenic temperatures (below − 150 °C) in order to prevent thermal runaway.

5.2. Repurposing: characterisation experiments

5.2.1. Capacity performance prior and after cryogenic freezing

Five capacity measurements are performed sequentially with 3 h rest in between each respective charge and discharge before the cells are submerged in LN_2 to ensure that the cells are working properly. This is shown in Fig. 7(a) for the DK 5 Ah cells and highlights there is little variation ($p_{value} = 0.87$) between capacity measurements for all sixteen cells after the first characterisation. The energy capacity measurements are circa 4% higher than the typical rated capacity of 5.5 Ah stated in the manufacturer's datasheet. The capacity measurements after the cells had been submerged in LN_2 are also summarised in Fig. 7(a) and show the capacities have been affected. For the DK 5 Ah cells submerged (yellow, red, and blue trace), there is a reduction in capacity after the first submersion in LN_2 (characterisation 6). However, there appears to be no further reduction in capacity for the subsequent LN_2 submersions (characterisation 7 and 8). This is confirmed by performing a two factor ANOVA with $p_{crit} = 0.05$, which shows that there is statistically significant difference between the different SOCs ($p_{value} = 4.85 \times 10^{-23} < 0.05$) but not between the number of submersions ($p_{value} = 0.12 > 0.05$). There is also no statistical significance in the interaction between SOC and the number of submersions

(p_{value} = 0.80 > 0.05). Fig. 7(a) shows that the degradation is correlated with the SOC: DK 5 Ah cells lost 1.1 ± 0.1%, 1.4 ± 0.1%, and 0.5 ± 0.1% capacity for 100%, 50%, and 0% SOC respectively when compared to the reference cells. Notably the behaviour of the reference cell, despite not being submerged in LN_2 demonstrates a small reduction in capacity (0.3 ± 0.1%) due to ageing effect of either cell electrical cycling or storage process.

The five capacity measurements performed sequentially before the Panasonic 3 Ah cells were submerged in LN_2 are shown in Fig. 7(b). As it can been seen, after the first characterisation, there is little variation between capacity measurements for all eighteen cells. A two factor ANOVA with p_{crit} = 0.05 was performed and confirms there is no statistical significance between the characterisations 2–5 (p_{value} = 0.08 > 0.05) and in the interaction between SOC and the characterisations 2–5 (p_{value} = 1.00 > 0.05). However, there is statistically significant difference between the different SOCs ($p_{value} = 9.0 \times 10^{-5} < 0.05$). This is an intuitive result since the Panasonic 3 Ah cells submerged at 100% SOC (blue trace) have consistently lower capacity than the remaining cells. The energy capacity measurements are close to the rated capacity of 3 Ah specified in the manufacturer's datasheet. The capacity measurements after the cells have been submerged LN_2 (characterisations 6–9) are also summarised in Fig. 7(b), which highlight the cell's respective capacities have been not been affected. A two factor ANOVA with p_{crit} = 0.05 was performed and confirms that there is no statistical significance between the number of submersions (p_{value} = 0.13 > 0.05) or in the interaction between SOC and the number of submersions (p_{value} = 0.36 > 0.05). However, as with the characterisations before cryogenic freezing, there is statistically significant difference between the different SOCs (p_{value} = 0.04 < 0.05). Post hoc testing reveals that there is no pair-wise statistically significant difference between the reference cells (purple trace) and each SOC (p_{value} at 100% = 0.03 > 0.008, p_{value} at 50% = 0.82 > 0.008, p_{value} at 0% = 0.44 > 0.008). The pair-wise statistically significant difference is between the Panasonic 3 Ah submerged at 100% SOC the group submerged at 50% SOC ($p_{value} = 2.09 \times 10^{-3} < 0.008$).

In summary, the DK 5 Ah cells lost 0.5–1.1% capacity after cryogenic freezing when compared to reference cells whereas the Panasonic 3 Ah did not suffer any statistically significant capacity loss.

5.2.2. HPPC

Fig. 8(a–c) shows that the DK 5 Ah HPPC measurements are grouped together for the first characterisation (prior to cryogenic freezing) and diverge for the subsequent characterisations (post cryogenic freezing). Single factor ANOVAs with p_{crit} = 0.05 performed on the DK 5 Ah first HPPC characterisation confirms that there are no statistically significant differences between the four cell groups prior to LN_2 submersions (p_{value} at 90% SOC = 0.99, p_{value} at 50% SOC = 0.99, p_{value} at 20% SOC = 0.91). Two factor ANOVAs with p_{crit} = 0.05 performed on the HPPC measurements at 90%, 50%, and 20% SOC are summarised in Table 3.

Table 3 shows that there is no statistically significant difference in the interaction between SOC groups and the number of LN_2 submersions for all the HPPC characterisations performed. There is however, statistically significant difference between SOC groups (i.e. submerged at 100%, 50%, and 0% SOC and the reference case) and between the number of LN_2 submersions for all the HPPC characterisations performed.

The post hoc testing results, performed using paired t-tests with Bonferroni correction, are shown in Table 4. Table 4 reveals that there is no pair-wise statistically significant difference between the reference cells (purple trace) and each SOC. The pair-wise statistically significant difference are between:

- the DK 5 Ah submerged at 0% SOC the group submerged at 100% SOC ($p_{value} = 3.5 \times 10^{-3} < 0.008$) and 50% SOC ($p_{value} = 9.4 \times 10^{-4} < 0.008$) for the HPPC performed at 90% SOC
- the DK 5 Ah submerged at 0% SOC the group submerged and 50% SOC ($p_{value} = 7.9 \times 10^{-4} < 0.008$) for the HPPC performed at 50% SOC
- the DK 5 Ah submerged at 100% SOC the group submerged and 50% SOC ($p_{value} = 1.4 \times 10^{-3} < 0.008$) for the HPPC performed at 20% SOC.

Table 4 also shows there is no pair-wise statistically significant difference between the first HPPC characterisation (prior to cryogenic freezing) and each subsequent HPPC characterisation after LN_2 submersion except between the first HPPC characterisation and the fourth HPPC characterisation performed at 20% SOC ($p_{value} = 2.6 \times 10^{-4} > 0.008$). There is small decrease in cell impedance of -0.36 ± 0.19 mΩ measured at 20% SOC after five LN_2 submersions. There is also pair-wise statistically significant differences between the DK 5 Ah second and fourth HPPC characterisations at all SOCs (p_{value} at 90% SOC = $4.3 \times 10^{-4} < 0.008$, p_{value} at 50% SOC = $8.0 \times 10^{-3} < 0.008$, p_{value} at 20% SOC = $7.7 \times 10^{-4} < 0.008$).

The HPPC measurements performed on the Panasonic 3 Ah cell at three different SOCs, 90%, 50%, and 20% are shown in Fig. 8(d)–(f) respectively. These show that the Panasonic 3 Ah HPPC measurements are grouped together for the first characterisation (prior to cryogenic freezing) and diverge for HPPC at 20% SOC (Fig. 8(f)) for the subsequent characterisations (post cryogenic freezing). Similarly, to the DK5 Ah cells, single factor ANOVAs with p_{crit} = 0.05 performed on the first Panasonic 3 Ah HPPC characterisation confirms that there are no statistically significant differences between the four cell groups prior to submersions (p_{value} at 90% SOC = 0.75, p_{value} at 50% SOC = 0.65, p_{value} at 20% SOC = 0.98). Two factor ANOVAs with p_{crit} = 0.05 performed on the HPPC measurements at 90%, 50%, and 20% SOC are summarised in Table 5.

Table 5 shows that there is no statistically significant difference between SOC groups (i.e. submerged at 100%, 50%, and 0% SOC and reference) and the interaction between SOC groups and the number of LN_2 submersions. There is however, statistically significant difference ($2.1 \times 10^{-5} < 0.05$) between LN_2 submersions for the HPPC characterisations performed at 20% SOC (Fig. 8(f)). The post hoc testing results, performed using paired t-tests with Bonferroni correction, are shown in Table 6.

Table 6 reveals that there is pair-wise statistically significant difference between the first HPPC characterisation (prior to cryogenic freezing) and:

- the 2nd characterisation (one LN_2 submersion - $p_{value} = 2.1 \times 10^{-3} < 0.008$)
- the 3rd characterisation (two LN_2 submersions - $p_{value} = 4.4 \times 10^{-3} < 0.008$)

Table 3
DK 5 Ah two factor ANOVA p-values for each SOC (p_{crit} = 0.05 – statically significant in bold).

DK 5 Ah	HPPC at 90% SOC	HPPC at 50% SOC	HPPC at 20% SOC
Between SOC	$\mathbf{p_{value} = 4.0 \times 10^{-5}}$	$\mathbf{p_{value} = 1.2 \times 10^{-3}}$	$\mathbf{p_{value} = 1.9 \times 10^{-3}}$
Between LN_2 submersions	$\mathbf{p_{value} = 8.0 \times 10^{-6}}$	$\mathbf{p_{value} = 0.01}$	$\mathbf{p_{value} = 9.4 \times 10^{-5}}$
Interactions between SOC and LN_2 submersions	p_{value} = 0.09	p_{value} = 0.46	p_{value} = 0.55

Table 4
DK 5 Ah post hoc testing: pair-wise *t*-test with Bonferroni correction (p_{crit} = 0.0083 – statistically significant in bold).

DK 5 Ah	Between SOC				Between LN_2 submersions			
	p_{value}	100%	50%	0%	p_{value}	2	3	4
HPPC at 90% SOC	**Ref**	0.04	0.02	0.20	**1**	0.03	0.44	0.02
	100%		0.88	**3.5×10^{-3}**	**2**		0.01	**4.3×10^{-4}**
	50%			**9.4×10^{-4}**	**3**			0.16
HPPC at 50% SOC	**Ref**	0.50	0.01	0.26	**1**	0.36	0.52	0.02
	100%		0.04	0.07	**2**		0.17	**8.0×10^{-3}**
	50%			**7.9×10^{-4}**	**3**			0.14
HPPC at 20% SOC	**Ref**	0.03	0.30	0.17	**1**	0.68	0.04	**2.6×10^{-4}**
	100%		**1.4×10^{-3}**	0.58	**2**		0.04	**7.7×10^{-4}**
	50%			0.02	**3**			0.07

- the 4th characterisation (five LN_2 submersions - $p_{value} = 1.5 \times 10^{-5} < 0.008$)

The difference from the reference cells after five LN_2 submersion is 4.7 ± 2.0 mΩ, 1.1 ± 1.8 mΩ, and 6.2 ± 2.8 mΩ for the Panasonic 3 Ah cells submerged in LN_2 at 100%, 50%, and 0% SOC respectively. This suggests that multiple flash freezing events only have a moderate impact on the Panasonic 3 Ah cell impedance: i.e. a 6.5 ± 2.8% increase if the cells are fully charged (100% SOC), and an 8.7 ± 3.9% increase if they are fully discharged (0% SOC) during the LN_2 submersion process.

In summary, the DK 5 Ah cells did not suffer any increase in impedance due to cryogenic freezing. For the Panasonic 3 Ah cells, the impedance measured at 90% and 50% SOC also did not increase. However, the Panasonic 3 Ah cells impedance measured at 20% SOC increased by 1.1–6.2% after cryogenic freezing when compared to reference cells.

The abuse experiments demonstrate that both cells types are not considerably damaged from cryogenic freezing, thereby facilitating repurposing of damaged or defective LIBs.

5.2.3. Voltage decay and recovery

As described in Section 3.4, the cell terminal voltage is recorded throughout the cryogenic freezing. The cells terminal voltage dropped to 0 V after they were submerged in LN_2 and returned to its previous value after the cells were removed from the LN_2 as shown in Fig. 9(a) and (b) respectively.

The cells were submerged in LN_2 at $t = 0$ s (Fig. 9(a)), and removed from LN_2 at $t = 0$ s (Fig. 9(b)). This confirms that the electrolyte was frozen and that there is no electromotive force across the cell terminals at cryogenic temperature. Fig. 9(a) shows that it takes the electrolyte of both cell types circa 120 s after LN_2 submersion to freeze (voltage = 0 V). This confirms that the five minutes LN_2 submersion time using for the experiments was sufficient to completely freeze the electrolyte.

As can be seen in Fig. 9(a), the terminal voltage of the DK 5 Ah cells (purple trace) was observed to decay circa 20 s sooner than the Panasonic 3 Ah cells (yellow, red and blue traces). Similarly, the DK 5 Ah cells terminal voltage (purple trace) rises circa 100 s before the Panasonic cells (yellow, red and blue traces) once removed from the LN_2 (Fig. 3b). This is an intuitive result since the DK 5 Ah cells have a surface area that is five times larger than the Panasonic 3 Ah cells (e.g. ~212cm^2 compared to 42 cm^2 – estimated using the cell dimensions), whilst only weighing two and half times as much (126.0 g vs 49.0 g). Therefore the DK 5 Ah should respond to temperature changes faster. Interestingly, there appears to be a correlation between SOC and the electrolyte freezing rate in the Panasonic 3 Ah cells. The charged cells (blue trace – 100% SOC) all freeze before the mid SOC cells (red trace – 50% SOC) and the discharge cells (yellow trace – 0% SOC). The time taken to reach 50% of the initial voltage is shown in Table 7.

Table 7 also shows the time taken to reach 50% voltage after the cells are removed from the LN_2 and reveals the correlation is less pronounced but still visible. It is suspected that this is due to increased thermal conductivity at higher SOC. While the electrolyte concentration remains constant irrespective of the SOC [72], the volume of the active materials increases at higher SOC, which could improve the contact between the electrodes, separators, and packaging and therefore increase the thermal conductivity. The fully charged cells (Panasonic 100% - blue trace in Fig. 9) appears to freeze sooner (the voltage decays before discharged cells). The rate at which the cell voltage decays and rises in the Panasonic 3 Ah cells appears to be the same regardless of the SOC at the point of freezing. In comparison to the DK 5 Ah cells, the voltage gradient is higher in the Panasonic 3 Ah cells suggesting that the manufacturers have used significantly different electrolyte compositions.

Table 6
Panasonic 3 Ah post hoc testing: pair-wise *t*-test with Bonferroni correction (p_{crit} = 0.0083 – statistically significant in bold).

Panasonic 3 Ah	Between LN_2 submersions			
	p_{value}	2	3	4
HPPC at 20% SOC	1	**2.1×10^{-3}**	**4.4×10^{-3}**	**1.5×10^{-5}**
	2		0.14	0.05
	3			0.99

5.3. Further work

Very little detrimental impact to cell performance was found even after five repetitive thermal cycles on two cell chemistries and form factors (18,650 energy NCA and small pouch power NMC). It is expected this applies to other Li-ion chemistries. Cell autopsies are to be performed in order to understand the potential mechanical deformations induced from the internal stresses caused by the materials with

Table 5
Panasonic 3 Ah two factor ANOVA p-values for each SOC.

Panasonic 3 Ah	HPPC at 90% SOC	HPPC at 50% SOC	HPPC at 20% SOC
Between SOC	$p_{value} = 0.11$	$p_{value} = 0.07$	$p_{value} = 0.11$
Between LN_2 submersions	$p_{value} = 0.56$	$p_{value} = 0.45$	$\mathbf{p_{value} = 2.1 \times 10^{-5}}$
Interactions between SOC and LN_2 submersions	$p_{value} = 0.67$	$p_{value} = 0.40$	$p_{value} = 0.65$

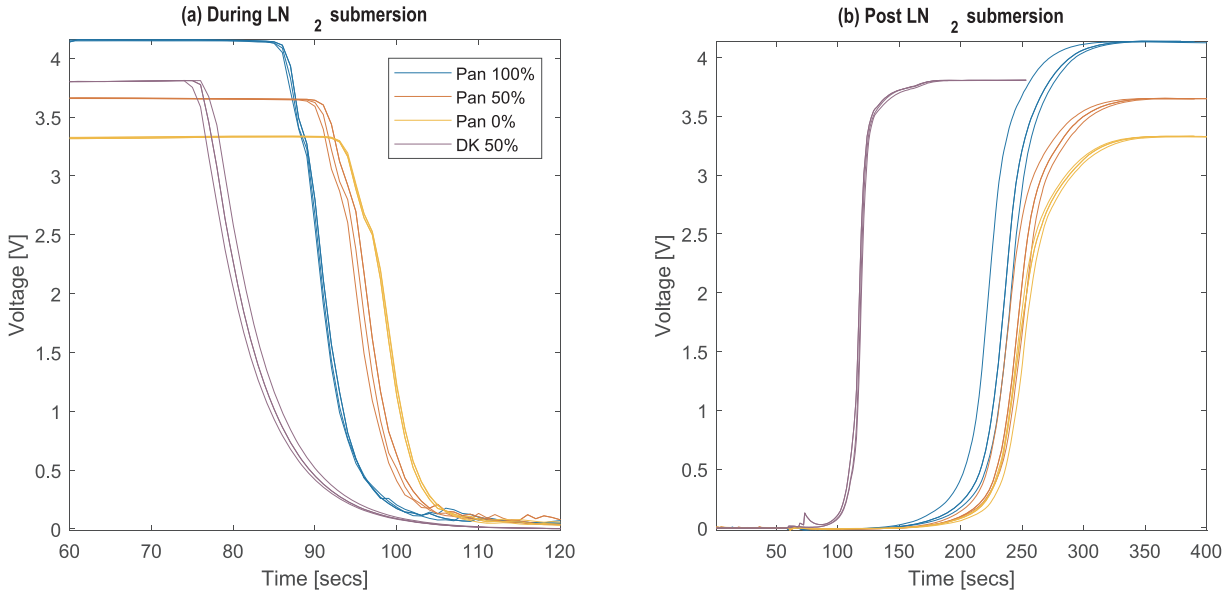

Fig. 9. Terminal voltage (a) during LN_2 submersion at t = 0 s and (b) after removal from LN_2 at t = 0 s.

Table 7
Time taken for cells to reach 50% initial voltage.

	Initial voltage	Final voltage	Time to 50% voltage	
			during LN_2 submersion	post LN_2 submersion
Pan 0%	3.32 V	3.32 V	99s	248.5s
Pan 50%	3.66V	3.66V	96.5s	247.5s
Pan 100%	4.16V	4.16V	91s	239s
DK 50%	3.80 V	3.80 V	81s	117s

different thermal coefficients of expansion discussed in Section 2.2.

Further work is being undertaken to demonstrate that cryogenically frozen and thawed cells perform similarly throughout the expected automotive lifecycle (20% capacity fade). Subsequently the work will be scaled form cell to module and pack level. Scenarios such as whether thermal runaway of a module or pack experiencing a fire can be supressed with cryogenic freezing will be considered. Since it is expected that it is not necessary to maintain the packs at cryogenic temperatures (below −150 °C) in order to prevent thermal runaway, experiments to establish the minimum temperature to prevent thermal runaway are also being undertaken. This will also involve investigating the ability and feasibility of recovering functional cells or modules from a damaged LIB pack.

Since the cylindrical cells did not go into thermal runaway, further work is being undertaken to improve the crushing experiment and insure the method causes internal short circuits. Finally, an investigation into how different freezing rates affect the results is being carried out with a view to elucidate the observation that higher SOCs caused the electrolyte to freeze at lower temperatures.

6. Conclusions

The abuse tests (short circuit and penetration) were selected as they are the most destructive abuse experiments for LIBs. The abuse testing results fulfil the first objective of this work since it establishes Li-ion cells are deemed safe when cryogenically cooled. This is because the electrolyte is frozen solid and does not permit any ions to mobilise therefore no current could flow even under the most extreme abuse conditions. Cryogenically cooled cells are unable to release any energy and the possibility of thermal runaway is removed. Cryogenically frozen LIBs are therefore not “liable to rapidly disassemble, dangerously react, produce a flame or dangerous evolution of heat or a dangerous emission of toxic, corrosive or flammable gases or vapours” (as per ADR [22]) and consequently could be transported safely without explosion proof containers.

The characterisation experiment evidences that there are no significant detrimental effects on cell performance of flash freezing Li-ion cells, thus fulfilling the second objective of this research. The cell performance was determined by its impedance and capacity, as these dictate the power delivery capability and the amount of energy that can be stored. Cell impedance and capacity were characterised before and after cryogenic freezing and thawing to quantify any low temperature effects on cell performance. Very little detrimental impact on cell performance was found even after five repetitive thermal cycles of cryogenic freezing and thawing on two cell chemistries and form factors (18,650 energy NCA and small pouch power NMC). Cryogenically freezing cells offers a prospective solution for safely transporting damaged LIBs or battery packs where it is not possible to determine the state of health. This may also facilitate reuse and remanufacture of LIBs, greatly prolonging the useful life, reducing the consumption of raw materials, and improving environmental sustainability.

This is a timely research subject aligned with plans for manufacturing and sustainability. The “triple win” report by the all-party Parliamentary Sustainable Resource Group and the All-Party Parliamentary Manufacturing Group highlights the social, economic and environmental case for remanufacturing [30]. It asserts that the future of the manufacturing industry is inextricably linked to environmental sustainability, reducing the consumption of raw materials, and exploiting new areas of comparative advantage, and that remanufacturing plays a critical role in this.

Acknowledgements

The research was undertaken as a part of ELEVATE project (EP/M009394/1) funded by the Engineering and Physical Science Research Council (EPSRC) and the WMG Centre High Value Manufacturing Catapult (funded by Innovate UK). This research was also supported by the Warwick Impact fund in collaboration with Jaguar Land Rover.

References

[1] The European Parliament and the Council of the European Union, ‘Regulation (EU)

No 333/2014 of the European Parliament and of the Council of 11 March 2014 Amending Regulation (EC) No 443/2009 to Define the Modalities for Reaching the 2020 Target to Reduce CO2 Emissions From New Passenger Cars', Off. J. Eur. Union L103 (2014) 15–21.
[2] J.H. Seinfeld, S.N. Pandis, Atmospheric Chemistry and Physics: From Air Pollution to Climate Change, John Wiley & Sons, Hoboken, NJ, USA, 2016.
[3] United States Department of Energy, 'One Million Electric Vehicles By 2015 Status Report Executive Summary', 2015.
[4] T.R.B. Grandjean, A. McGordon, P. Jennings, Structural identifiability of equivalent circuit models for Li-ion batteries, Energies 10 (January (1)) (2017).
[5] Eurostat, Greenhouse Gas Emission Statistics – Statistics Explained, [Online]. Available: (2017) Accessed 30 November 2017 http://ec.europa.eu/eurostat/statistics-explained/index.php/Greenhouse_gas_emission_statistics#Further_Eurostat_information.
[6] European Commission, The Roadmap for Transforming the EU into a Competitive, Low-Carbon Economy by 2050, (2011).
[7] K.E. Aifantis, S.A. Hackney, R.V. Kumar, Wiley InterScience (Online service), High Energy Density Lithium Batteries: Materials, Engineering, Applications, John Wiley & Sons, Hoboken, NJ, USA, 2010.
[8] The Boston Consulting Group Inc, Batteries for Electric Cars; Challenges, Opportunities, and the Outlook to 2020, (2016) [Online]. Available: http://www.bcg.com/documents/file36615.pdf Accessed 2 December 2016.
[9] Bloomberg New Energy Finance, 'Electric Vehicle Outlook 2017', 2017. [Online]. Available: https://about.bnef.com/electric-vehicle-outlook/. (Accessed 4 December 2017).
[10] K.S. Ng, C.-S. Moo, Y.-P. Chen, Y.-C. Hsieh, Enhanced coulomb counting method for estimating state-of-charge and state-of-health of lithium-ion batteries, Appl. Energy 86 (September (9)) (2009) 1506–1511.
[11] Y. Zou, X. Hu, H. Ma, S.E. Li, Combined State of Charge and State of Health estimation over lithium-ion battery cell cycle lifespan for electric vehicles, J. Power Sources 273 (January) (2015) 793–803.
[12] M. Berecibar, I. Gandiaga, I. Villarreal, N. Omar, J. Van Mierlo, P. Van den Bossche, Critical review of state of health estimation methods of Li-ion batteries for real applications, Renew. Sustain. Energy Rev. 56 (April) (2016) 572–587.
[13] D.P. Abraham, J.L. Knuth, D.W. Dees, I. Bloom, J.P. Christophersen, Performance degradation of high-power lithium-ion cells—electrochemistry of harvested electrodes, J. Power Sources 170 (2) (2007) 465–475.
[14] M. Broussely, et al., Main aging mechanisms in Li ion batteries, J. Power Sources 146 (1) (2005) 90–96.
[15] H. Yamada, Y. Watanabe, I. Moriguchi, T. Kudo, Rate capability of lithium intercalation into nano-porous graphitized carbons, Solid State Ionics 179 (27) (2008) 1706–1709.
[16] S. Saxena, C. Le Floch, J. MacDonald, S. Moura, Quantifying EV battery end-of-life through analysis of travel needs with vehicle powertrain models, J. Power Sources 282 (2015) 265–276.
[17] T. Grandjean, et al., Accelerated internal resistance measurements of lithium-ion cells to support future end-of-life strategies for electric vehicles, Batteries 4 (October (4)) (2018) 49.
[18] Y.-H. Chiang, W.-Y. Sean, C.-H. Wu, C.-Y. Huang, Development of a converterless energy management system for reusing automotive lithium-ion battery applied in smart-grid balancing, J. Clean. Prod. 156 (July) (2017) 750–756.
[19] L. Gaines, The future of automotive lithium-ion battery recycling: charting a sustainable course, Sustain. Mater. Technol. 1–2 (December) (2014) 2–7.
[20] J. Groenewald, T.R.B. Grandjean, J. Marco, Accelerated energy capacity measurement of lithium-ion cells to support future circular economy strategies for electric vehicles, Renew. Sustain. Energy Rev. 69 (2017) 98–111.
[21] L.A.-W. Ellingsen, C.R. Hung, A.H. Strømman, Identifying key assumptions and differences in life cycle assessment studies of lithium-ion traction batteries with focus on greenhouse gas emissions, Transp. Res. Part D: Transp. Environ. 55 (August) (2017) 82–90.
[22] Economic Commission for Europe Inland Transport Committee, 'European Agreement Concerning the International Carriage of Dangerous Goods by Road', vol. 1. 2017.
[23] The European Parliament and the Council of the European Union, Directive 2006/66/EC on batteries and accumulators and waste batteries and accumulators, Off. J. Eur. Union (2006).
[24] 'Verpackungsgruppe I – Brandschutz durch Pyrobubbles'. [Online]. Available: https://www.genius-group.de/produkte/pyrobubbles-lionguard-lithium-ionen-batterien/verpackungsgruppe-1/. (Accessed: 02 October 2018).
[25] X. Zeng, J. Li, N. Singh, Recycling of spent lithium-ion battery: a critical review, Crit. Rev. Environ. Sci. Technol. 44 (May (10)) (2014) 1129–1165.
[26] W. Lv, Z. Wang, H. Cao, Y. Sun, Y. Zhang, Z. Sun, A critical review and analysis on the recycling of spent lithium-ion batteries', ACS Sustain. Chem. Eng. 6 (February (2)) (2018) 1504–1521.
[27] M.O. Ramoni, H.-C. Zhang, End-of-life (EOL) issues and options for electric vehicle batteries, Clean Technol. Environ. Policy 15 (December (6)) (2013) 881–891.
[28] M. Foster, P. Isely, C.R. Standridge, M.M. Hasan, Feasibility assessment of remanufacturing, repurposing, and recycling of end of vehicle application lithium-ion batteries, J. Ind. Eng. Manag. JIEM 3 (2014) 2014–2017.
[29] C. Standridge, Remanufacturing, Repurposing, and Recycling of Post-Vehicle-Application Lithium-Ion Batteries, (2014).
[30] A.-M. Benoy, L. Owen, M. Folkerson, Triple Win: The Social, Economic and Enviromental Case for Remanufacturing, (2014).
[31] Environment Agency, Waste Batteries and Accumulators: Technical Guidance – GOV.UK, (2014) [Online]. Available: (Accessed 4 December 2017) https://www.gov.uk/guidance/waste-batteries-and-accumulators-technical-guidance#definitions.
[32] Q. Wang, P. Ping, X. Zhao, G. Chu, J. Sun, C. Chen, Thermal runaway caused fire and explosion of lithium ion battery, J. Power Sources 208 (2012) 210–224.
[33] S. Al Hallaj, H. Maleki, J.S. Hong, J.R. Selman, Thermal modeling and design considerations of lithium-ion batteries, J. Power Sources 83 (1) (1999) 1–8.
[34] H. Maleki, G. Deng, A. Anani, J. Howard, Thermal stability studies of li-ion cells and components, J. Electrochem. Soc. 146 (9) (1999) 3224.
[35] I. – International Energy Agency, 'Global EV Outlook 2017 Together Secure Sustainable Global EV outlook 2017'.
[36] X. Zeng, J. Li, L. Liu, Solving spent lithium-ion battery problems in China: opportunities and challenges, Renew. Sustain. Energy Rev. 52 (December) (2015) 1759–1767.
[37] D. Lisbona, T. Snee, A review of hazards associated with primary lithium and lithium-ion batteries, Process Saf. Environ. Prot. 89 (November (6)) (2011) 434–442.
[38] C. Hand, 'Dealing with waste lithium batteries | Croner-i', 2013. [Online]. Available: https://app.croneri.co.uk/feature-articles/dealing-waste-lithium-batteries-0#WKID-20131001105801058610586-01769310 (Accessed: 01-Dec-2017).
[39] United Nations, 'Recommendations on the TRANSPORT OF DANGEROUS GOODS Model Regulations Volume I', 2017.
[40] United Nations, Recommendations on the Transport of Dangerous Goods: Manual of Tests and Criteria, 5th edition, (2009).
[41] NFPA, 'Alternative Fuel Vehicles Safety Training Program - NFPA', 2015. [Online]. Available: http://www.nfpa.org/training-and-events/by-topic/alternative-fuel-vehicle-safety-training (Accessed: 05-Dec-2017).
[42] C. Williams, Man hospitalised in battery recycling plant explosion | News | Materials Recycling World', 2017. [Online]. Available: https://www.mrw.co.uk/latest/man-hospitalised-in-battery-recycling-plant-explosion/10020183.article (Accessed: 30-Nov-2017).
[43] E. Cabrera-Castillo, F. Niedermeier, A. Jossen, Calculation of the state of safety (SOS) for lithium ion batteries, J. Power Sources 324 (August) (2016) 509–520.
[44] A. Sonoc, J. Jeswiet, V.K. Soo, Opportunities to improve recycling of automotive lithium ion batteries, Procedia CIRP 29 (January) (2015) 752–757.
[45] T. Georgi-Maschler, B. Friedrich, R. Weyhe, H. Heegn, M. Rutz, Development of a recycling process for Li-ion batteries, J. Power Sources 207 (June) (2012) 173–182.
[46] E. Martinez-Laserna, et al., Evaluation of lithium-ion battery second life performance and degradation, 2016 IEEE Energy Conversion Congress and Exposition (ECCE), (2016), pp. 1–7.
[47] P. Zhang, T. Yokoyama, O. Itabashi, T.M. Suzuki, K. Inoue, Hydrometallurgical process for recovery of metal values from spent lithium-ion secondary batteries, Hydrometallurgy 47 (January (2–3)) (1998) 259–271.
[48] R. Gupta, A. Manthiram, Chemical extraction of lithium from layered LiCoO2, J. Solid State Chem. 121 (February (2)) (1996) 483–491.
[49] B. Swain, Recovery and recycling of lithium: a review, Sep. Purif. Technol. 172 (January) (2017) 388–403.
[50] W. McLaughlin and T. S. Adams, 'Li reclamation process', US5888463 A, 1998.
[51] William J. McLaughlin, 'Method for the neutralization of hazardous materials', US5345033 A, 23-Dec-1992.
[52] K.L. Gering, Low-temperature performance limitations of lithium-ion batteries, ECS Trans. 1 (26) (2006) 119–149.
[53] C.-K. Huang, J.S. Sakamoto, J. Wolfenstine, S. Surampudi, The limits of low-temperature performance of Li-Ion cells, J. Electrochem. Soc. 147 (August (8)) (2000) 2893.
[54] Y. Ji, Y. Zhang, C.-Y. Wang, Li-ion cell operation at low temperatures, J. Electrochem. Soc. 160 (February (4)) (2013) A636–A649.
[55] Y. Ein-Eli, S.R. Thomas, R. Chadha, T.J. Blakley, V.R. Koch, Li-ion battery electrolyte formulated for low-temperature applications, J. Electrochem. Soc. 144 (March (3)) (1997) 823.
[56] B.K. Mandal, A.K. Padhi, Z. Shi, S. Chakraborty, R. Filler, New low temperature electrolytes with thermal runaway inhibition for lithium-ion rechargeable batteries, J. Power Sources 162 (November (1)) (2006) 690–695.
[57] S. Li, X. Li, J. Liu, Z. Shang, X. Cui, A low-temperature electrolyte for lithium-ion batteries, Ionics (Kiel) 21 (April (4)) (2015) 901–907.
[58] M. Kasprzyk, A. Zalewska, L. Niedzicki, A. Bitner, M. Marcinek, W. Wieczorek, Non-crystallizing solvent mixtures and lithium electrolytes for low temperatures, Solid State Ionics 308 (October) (2017) 22–26.
[59] M. Petzl, M. Kasper, M.A. Danzer, Lithium plating in a commercial lithium-ion battery – a low-temperature aging study, J. Power Sources 275 (2015) 799–807.
[60] R.P. Day, et al., Differential thermal analysis of Li-ion cells as an effective probe of liquid electrolyte evolution during aging, J. Electrochem. Soc. 162 (January (14)) (2015) A2577–A2581.
[61] F. Pobell, Matter and Methods at Low Temperatures, Springer, 2007.
[62] M.S. Ding, K. Xu, T.R. Jow, Liquid-solid phase diagrams of binary carbonates for lithium batteries, J. Electrochem. Soc. 147 (May (5)) (1688) 2000.
[63] M.S. Ding, K. Xu, S. Zhang, T.R. Jow, Liquid/solid phase diagrams of binary carbonates for lithium batteries part II, J. Electrochem. Soc. 148 (April (4)) (2001) A299.
[64] International Electrotechnical Commission (IEC), IEC 62660-1 Secondary Lithium-Ion Cells for the Propulsion of Electric Road Vehicles – Part 1: Performance Testing'. Geneva, Switzerland, 2010, (2010).
[65] D.H. Doughty, C.C. Crafts, FreedomCAR Electrical Energy Storage System Abuse Test Manual for Electric and Hybrid Electric Vehicle Applications, (2006).
[66] K.-C. Chiu, C.-H. Lin, S.-F. Yeh, Y.-H. Lin, K.-C. Chen, An electrochemical modeling of lithium-ion battery nail penetration, J. Power Sources 251 (April) (2014) 254–263.
[67] INL, 'Battery Test Manual for Plug-In Hybrid Electric Vehicles'. 2010.
[68] A. Barai, K. Uddin, W.D. Widanage, A. McGordon, P. Jennings, Comparison of

characterisation methodologies of internal impedance of lithium-ion cell and their interpretation, Appl. Energy Under Rev. (2016).
[69] R. Zhao, J. Liu, J. Gu, Simulation and experimental study on lithium ion battery short circuit, Appl. Energy 173 (July) (2016) 29–39.
[70] F. Larsson, P. Andersson, P. Blomqvist, B.-E. Mellander, Toxic fluoride gas emissions from lithium-ion battery fires, Sci. Rep. 7 (December (1)) (2017) 10018.
[71] C. Mikolajczak, P. Michael Kahn, K. White, and R. Thomas Long, 'Lithium-Ion Batteries Hazard and Use Assessment Final Report'.
[72] C. Liu, Z.G. Neale, G. Cao, Understanding electrochemical potentials of cathode materials in rechargeable batteries, Mater. Today 19 (March (2)) (2016) 109–123.